ISSN: 1074-133X Vol 32 No. 10s (2025)

Using Multi-Scale Features, Hierarchical and Contour Covid Bodies Can Be Extracted from Bioinformatics Images

R Ashok Kumar¹, Shaheda Akthar²

¹ Research Scholar, Dept. of CSE, Acharya Nagarjuna University, Guntur, AP & Lecturer in Computer Science, SCIM Government College (A), Tanuku, West Godavari, AP, India

² Dr. Shaheda Akthar, Lecturer in Computer Science, Government College for Women (A), Guntur & Research Supervisor, Dept. of CSE, Acharya Nagarjuna University, Guntur, AP

Article History:

Received: 12-01-2025

Revised: 15-02-2025

Accepted: 01-03-2025

Abstract:

The primary objective of processing and analyzing medical covid images is to effectively extract covid body features from objects in the images, and a crucial part of this process is segmenting the bodies in the images. Allocation of covid resources, evaluation of ecological services, protection of covid resources monitoring system, and identification of flood disaster applications are all examples of real-time uses for this fundamental activity. Randomly extracting COVID bodies sfrom medical COVID images is a new challenge for image and COVID interpretation. Several covid applications have shown promise in using convolutional neural networks (CNN) to process this task efficiently. For effective covid segmentation from Bioinformatics COVID-19 pictures, several CNN-based methods have been suggested. When it comes to segmenting covid extraction from human medical images, multi scale covid extraction (MWEN) is the one convolutional neural network approach to extract covid part from medical images. Unfortunately, the large number of training sensing image samples and sparse arrangement of boundary pixels make it unsuitable for investigating automatic extraction of COVID body segmentation from medical COVID images. The purpose of this proposal is to present a new hierarchical neural network called NOMFCHNN that is optimized for multiple features to improve the stage of autonomous body segmentation from medical COVID images. Using pixel matching and extended feature extraction, NOMFCHNN builds a neural network with features that expand and inception-related layers that store network localization data. By utilizing contour map optimization, this method can also detect contours using globalized images and segmentation. It then passes the result of each contour identification into the next contour identification in the chosen hierarchical area. In addition, our suggested method checks the low-resolution term for every pixel in the picture, learning the image from the segmentation results of nearby pixels to get rid of inaccuracies or minor modifications. To evaluate the feature extraction of covid body from human medical covid images, we choose a multi-scale feature segmentation fusion module to better recognize the outlines of the COVID-19 body from the COVID-19 image. Comparing state-of-the-art procedures to those conducted on Bioinformatics Covid pictures, extensive trials on combined medical covid repository photos show that the suggested methodology enhances segmentation accuracy and other characteristics.

Keywords: Image segmentation, contour map optimization, Bioinformatic Covid images, extraction of covid body, CNN, MSFE, high and low pixel resolution

ISSN: 1074-133X Vol 32 No. 10s (2025)

1. Introduction

Emerging technology that relies on high-resolution medical COVID-19 footage is cutting edge. Collecting various forms of unidentified area-related photographs poses a new problem for workers in the field of geographic information systems. Digital mapping, urbanization monitoring, and medical covid picture interpretation are just a few examples of the many uses for this new area of study in covid. In the realm of covid resource monitoring, the extraction of COVID-19 bodies from bioinformatic COVID pictures is a novel and important idea. In the current real-time setting, segmentation/classification for COVID-19 body extraction is vital since COVID bodies change their environments. Figure 1 shows the representation of bodies of covid in bioinformatic Covid pictures based on higher end resolutions. Some of these images are blurry or deteriorated. The aquatic vitiation of silts, boat obstructions, and shadow cast by nearby tail plants are all causes of degradation in covidbody resources.

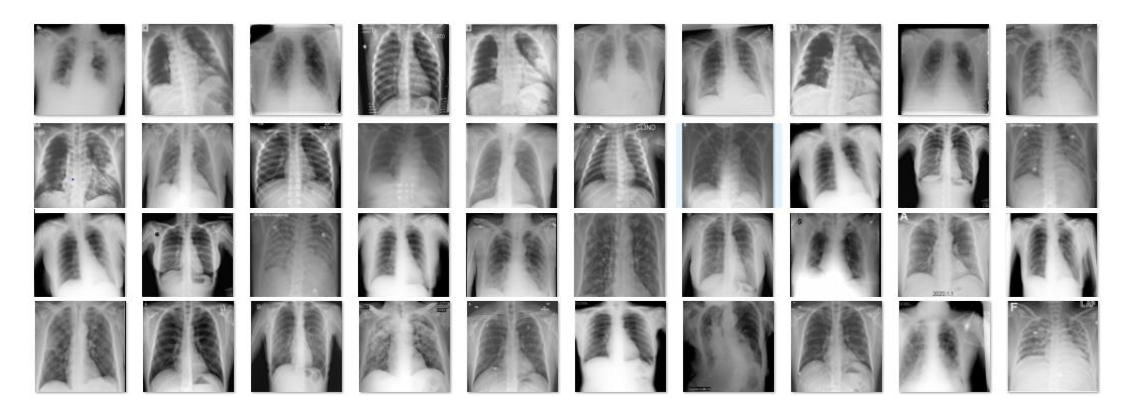


Figure 1: some of the typical and aerial medical covid images with sample covid bodies

Deep learning has been more popular among image processing techniques in recent years (Ref [16, 17]). Applications of convolutional neural networks (CNNs) include object detection [20, 21], semantic segmentation [19], and scene categorization [18, 19]. According to reference [22], CNNs can directly extract features from raw images by employing several convolutional layers, hence avoiding complex feature extraction. Pixel-by-pixel image categorization is one of CNNs' semantic segmentation capabilities that is used to extract information from COVID-19 images. Convolutional neural networks (CNNs) use deep convolutional layers to assign labels to pixels after recording pixel positions using shallow convolutional layers, as per ref [22]. A convolutional neural network (CNN) has three layers: two convolutional and one fully connected. The shallow structure of the system leads to its poor robustness in complex settings, as it can only capture low-level properties. Furthermore, a lot of papers use small input sizes for CNN models, so they are not appropriate for large-scale feature extraction. As the spatial resolution of medical COVID images increases, a number of deep learning-based methods for COVID body extraction have been proposed [25].CNNs are increasingly being utilized to extract data from COVID-19 images of infected people's bodies. In [10], an innovative application of CNN for COVID body extraction from Landsat ETM+ images was described. In a CNN technique, combining the super pixel is recommended in [6]. The core of this strategy consists of fusing artificially-designed traits with CNN-extracted ones. However, as forward propagation proceeds, certain crucial information is lost, which reduces the fluidity of covid extraction.

Recent years have seen advancements in fully convolutional neural networks (FCNs) and other end-to-end CNNs [26]. Beginning with semantic segmentation, the first end-to-end CNN was the fully convolutional network (FCN) [19]. Once the last convolutional layer has extracted abstract features from the input picture, FCN assigns labels to each pixel in the feature maps. On the other side, information associated with low-level features retrieved from the shallow convolutional layer is lost by FCN. Various models have been created to enhance CNN performance in computer vision's semantic segmentation in the past few years. Two examples are Unet (Ref. 23) and Deeplab V3+ (Ref. 24). The efficiency and precision of the covid body extraction were much enhanced after the implementation of these end-to-end CNNs. Employing CNNs for covid body extraction presents a number of

ISSN: 1074-133X Vol 32 No. 10s (2025)

difficulties. Forward propagation loses fine-grained covid body information due to the repeated max-pooling layers reducing the feature map resolution. In addition, feature maps with distinct pixel receptive fields enable feature information storage at multiple scales; this is because feature maps produced at different depths by convolutional layers [22] are not the same. Merging characteristics extracted at different scales in covid body extraction is an area that is now under-researched.

As for classification [21,22], building detection [23-25], road detection [26-28], and covid body extraction [21,23,29], several researchers have developed variants of U-net for different covid applications. Zhang, Z. [18] states that extremely high-resolution images of covid can have their bodies extracted using a deep convolutional encoder-decoder (DCED) architecture. Deep Unet, on the other hand, foresaw up sampling-induced blurring of the COVID-19 boundary pixels as a source of inaccurate results. A model called fully connected CRF (FCCRF) was employed to reduce the blurring effect [30]. The local structure information of the covid body and its boundary pixels were lost by FCCRF as a result of the smoothing effect [20]. The answer to the problem was the use of regional restriction (RR) and increased COVID body borders, which helped with prediction. A and Ronneberger O proposed in their 2015 and 2019 papers, respectively, the use of TernausNet for covid body segmentation [23]. The number 33, where a knowledge-transfer model was used to link tagged, high-resolution images. Disappointing prediction results are a result of the disparity in the spatial and spectral information distribution between high resolution and ultra-high resolution images. This defect causes the model to wrongly segment scenes that contain COVID-19 entities with differing spectral properties, in addition to failing to segment on many occasions. Transferring knowledge from high-resolution to very high-resolution photos did not enhance the efficiency or effectiveness of the segmentation. Although the majority of the aforementioned designs demonstrated outstanding performance, the computational complexity was increased due to the large number of trainable parameters. Both Ronneberger et al. [24] and H. Xiangyun et al. [25] laid the groundwork for the W-Net that is now being considered. Its superior performance allows it to compete with other techniques, such as the one proposed by Meng Chen et al. [23].

However, because of the uneven alignment of boundary pixels and the huge number of COVID training picture samples, there is insufficient data to investigate the automatic extraction of COVID body segmentation from medical COVID images. To improve the efficiency of automatic body segmentation using medical COVID images, we present an innovative optimized multi-feature contour-based hierarchical neural network (OMFCHNN). OMFCHNN finds the network's position by extracting features using an enlarged neural network layer. Enhanced feature extraction and pixel matching are the backbone of the suggested method. Another method that uses picture globalization to find contours is contour map optimization. The segmentation step of this approach uses a predefined hierarchical region to pass the results of one contour detection stage onto the next. In studies employing real-time bioinformatic COVID-19 pictures, the suggested method achieves high levels of accuracy in medical image segmentation based on recall, precision, and other metrics. What the proposed approach basically does is add:

- i) COVID pictures captured in difficult environments should be processed using feature extraction at high resolution and across multiple scales in order to recover covidbodies. The basic picture of encoding and decoding in convolutional neural network (CNN) feature extraction is combined with responsive feature data from lower and higher level pixels to build an ideal multi-scale feature.
- ii) For fine-grained COVID body scanning, we present a multi-scale feature extraction method based on optimized contour detection, with the aim of exploring the feasibility of enhancing the segmentation results from different labels.
- iii) We proposed an associative pixel matching-based COVID-19 body segmentation approach to improve performance.
- iv) Using an optimized pixel connection approach, we classify the segmented picture with outline COVID-19 body by evaluating the foreground and background image pixel processes.

ISSN: 1074-133X Vol 32 No. 10s (2025)

2. Materials and Methods

2.1. Area of Study

In this part, we will go over the groundwork for medical COVID-19 body extraction segmentation. In order to process heterogonous features in identification of sampled binary images and multi feature labelled covid body segmented images, the suggested work builds on top of convolutional neural networks with optimal characterization of multi features.

2.1.1. Feature extraction using several scales

For a multi-featured mixed network, three distinct models are described: RLFE (receptive longer feature extraction), CFE (channel-based feature extraction), and LFE (feature extraction on local variables). By utilizing LFE and RLFE, we define the spatial relationship between linked features and investigate the maximum features generated by cross-channel feature connections. Figure 2 depicts a beginner's attempt at multi-scale feature exploration.

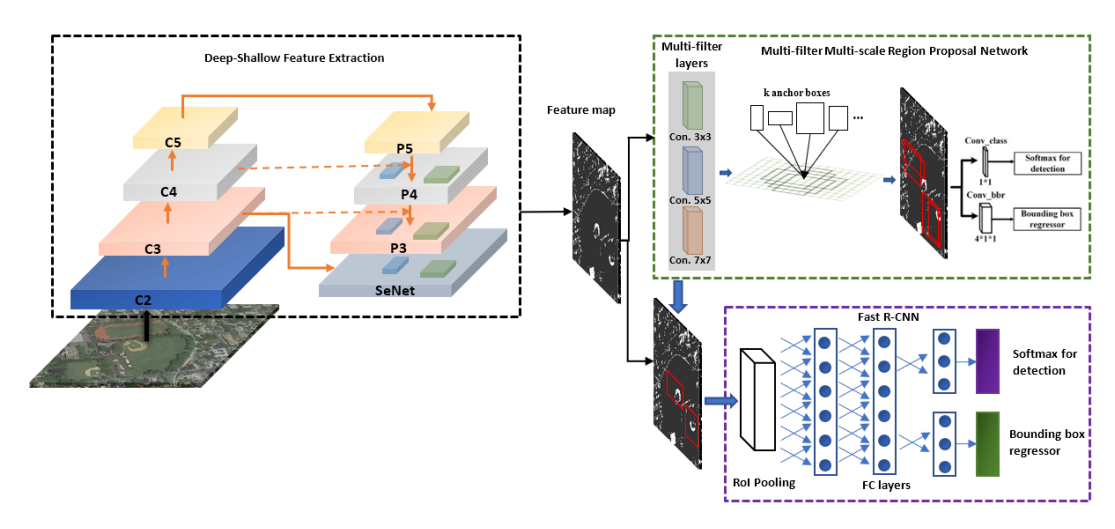


Figure 2. Multi-scale feature extraction procedure represented using various models.

Image pixel local data and feature map links were the basis of LFE design. It measures the separation between the weighted map connection and all local pixel features. The output of the current layer of the neural network is the input to the resultant distance. RLFE defines the kernel-associated function-based receptive big feature structure as

$$MRF = I + (I-1)*(d-1)$$

Amount of receptive features in terms of associative kernel sizes I obtained data from multiple layers of features after performing on neural convolution layers. Exploring global data from several pixel positions in an intense gradient image is described by CFE.

2.1.2. Contour Map Optimization

The topic of contour identification from images using localization image components has sparked discussions about several existing methods. We address here the topic of medical COVID-19 optimized contour detection using multi-scale globalization in conjunction with semantic picture data, such as texture, colour, form, and brightness.

Cb is the sub part of image weight with gradient G(a,b,o) from extensive medical covid image.

ISSN: 1074-133X Vol 32 No. 10s (2025)

Assume I is the intense medical COVID-19 image, and Cb is the contour block with the gradient signal $G(a,b,\theta)$

$$\chi^{2}(h,g) = \frac{1}{2} \sum_{k} \frac{\left(h(k) - g(k)\right)^{2}}{\left(h(k) - g(k)\right)}$$

The intensive image with locations a and b needs to be investigated and assessed using two subsample images, such as gradient mask and histogram images. Figure displays a sample representation of contour detection

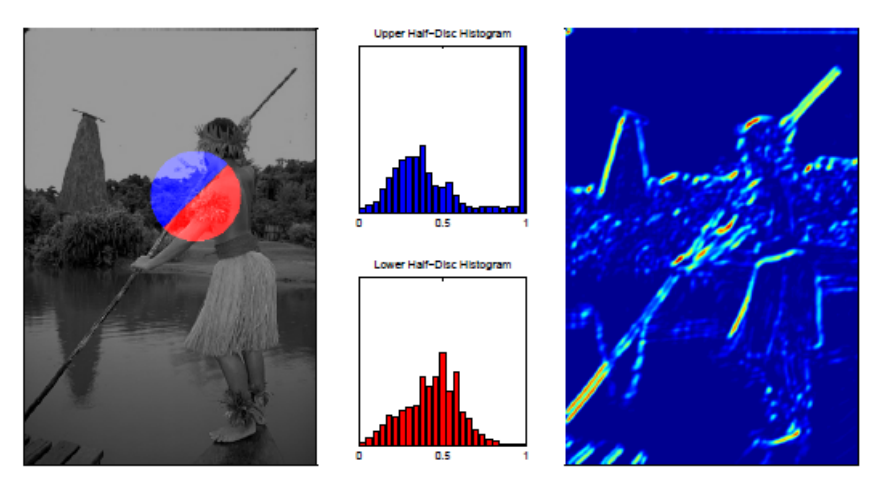


Figure 3. Contour representation from a sample-intensive image.

Figure 3 illustrates a contour map that goes along with an intense image; it uses deep layer functions to detect contours based on the three-dimensional localization of various components. This method, when applied to features with multiple labels and built on multi-scale contour detection,

$$mC_b(a,b,\theta) = \sum_{s} \sum_{k} \alpha_{k,s} G_{k,\sigma(k,s)}(a,b,\theta)$$

The computational process of the selected intensive image with locations a and b must be examined and evaluated with the use of two subsample photos, such as gradient mask images and histograms. An illustration of contour detection is shown in the image.

Let s represent the pixel's feature index and k stand for the feature's color, texture, and form representation i.e. $G_{k,\sigma(k,s)}$ & (a,b,θ) . Between related pixel notations in images, there is a histogram and a binary map mask image. The definition of ideal contour selection for a pixel in a picture is

$$OCM_{k,l} = \exp\left(\max_{p \in k,l} (mC_b(a)) / p\right)$$

In this case, k and l are pixel functions that are related with each other via associative distance; MSFE describes the optimal functionality of contour map detection. Apply this method to the suggested strategy.

2.2. A Novel Hierarchical Optimized Multi-Feature Contour Neural Network

In this part, we present a novel approach to deep segmentation that is both interactive and made possible by an optimized multi-feature contour-based hierarchical neural network (NOMFCHNN) and applied to high-resolution medical COVID images.

ISSN: 1074-133X Vol 32 No. 10s (2025)

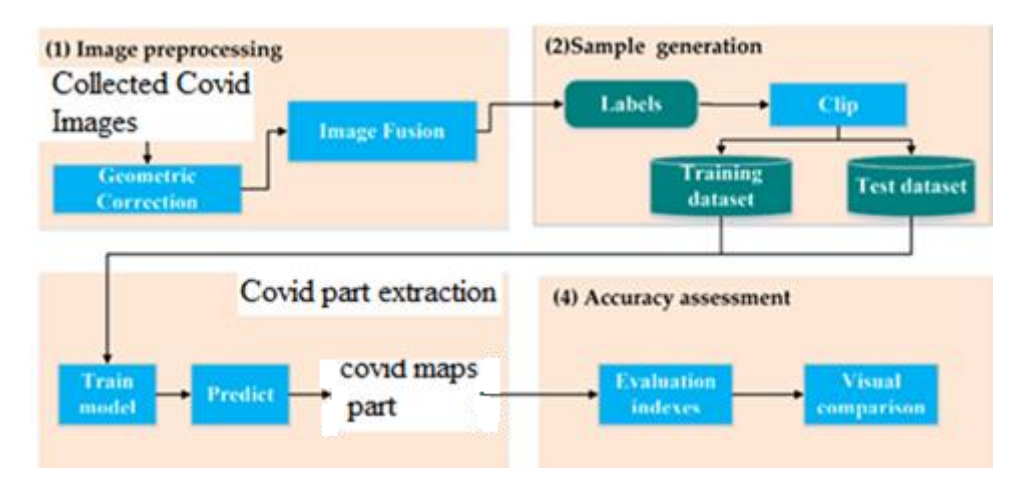


Figure 4. Process of the proposed technique.

The three main components of the suggested strategy are illustrated in Figure 4, which details its basic procedure: Enhancing the extraction of covid body segmentation, generalizing mapped picture collection based on guidance, and contour-based multi-scale feature extraction.

2.2.1. A collection of generalizable images based on guidelines

Using convolutional neural network (CNN) interactions, we transmit picture data into various binary sample images to generate pixel mapped image collections. A big number of training sample photos and map connections between sampling images are necessary for the data technique utilized in this paper, which is connected to deep learning images. All the many kinds of covid are represented in the image, which is a set of pixel labels. There is a visual interpretation that may be used to depict all the labels in medical COVID images, which consist of bodies of covid and backgrounds. Included in these photographs are both training and testing sets and they including every possible kind of covid. These samples include all pixels with a covid surface and some without. Almost every sampled library storage contains 14,000 to 15,000 samples from input trained images.

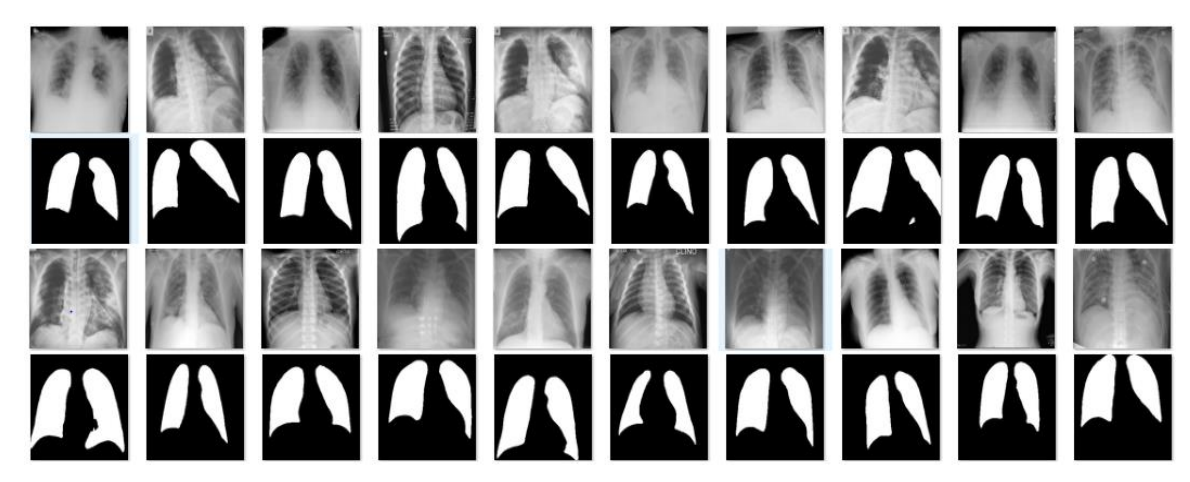


Figure 5 Medical covid images with passive and negative labeled samples.

Euclidean distance (DA) is a technique that we employ to move all the labeled samples to the set of guiding image maps. Every pixel in the trained sample picture is evaluated for DA at coordinates (k,l). The image's relevance map (uk,l), which is between [1,0] after that, is normalised. Our last section explains the relevance map for guidance as

ISSN: 1074-133X Vol 32 No. 10s (2025)

$$E(u_{k,l}) = 1 - \frac{1}{2} \left(DA_p(u_{k,l}) + DA_n(u_{k,l}) \right)$$

$$DA_{p}(u_{k,l}) = \min_{\forall u_{n,m} \in S_{p}} \sqrt{(k-n)^{2} + (l-m)^{2}}$$

$$DA_n(u_{k,l}) = \min_{\forall u_{n,m} \in S_n} \sqrt{(k-n)^2 + (l-m)^2}$$

 DA_p be the location of passive pixel, DA_n be the location of negative pixel and $u_{k,l}$ stand for the values of the pixels in the active and negative pixels areas, S represents the collection of pixels under consideration, and m and n stand for the random parameters. Consider evaluating global distance transformation (GDT) using encode and decode transforms based on user interactions to obtain the entire pixel distance of a picture.

$$GDT(u_{k,l}) = \min_{\forall u_{n,m} \in S_T} Dis(u_{k,l}, u_{n,m}, I), T \in (n, p)$$

$$Dis(u_{k,l}, u_{n,m}, I) = \min_{\forall path \in path_{n,m}} \int_{1} || \Delta I(path(s) * r(s)) || ds$$

Figure 6 illustrates the picture (I), path (r), and all paths found in the n, m parametric pixels (u, v), along with the vector of direct and gradient distances between these pixels, to accompany the execution of the sample guiding image.



Figure 6. DA-based picture, guiding map, passive label sampling, negative sampling, and image with sampling

After creating a binary sampled mask image using various pixel notations set to 1, 0, we tested multi-scale feature processing using sampling.

2.2.2. Differential feature extraction based on contours

The proposed contour-based multi-feature extraction is very different from the existing multi-scale extraction features; so, we employ the following modules to process it: extraction of local features (LFE), channel and long receptive field-based feature extraction (CFE&LRFE), and so on. CFE investigates information regarding the connections between several feature maps, whereas LFE and LRFE are components utilized for feature-based region selection.

ISSN: 1074-133X Vol 32 No. 10s (2025)

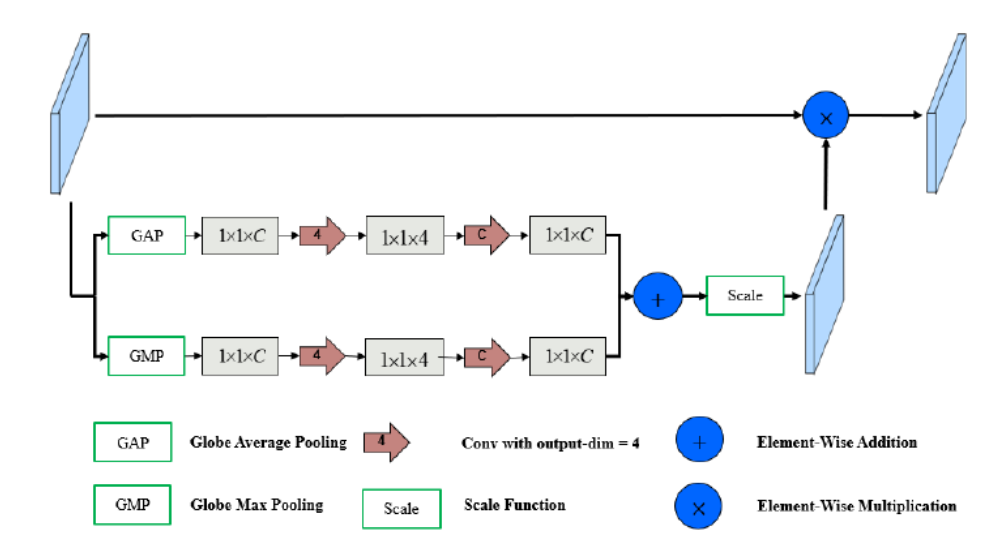


Figure 7 shows a representation of the AGC module using convolution layers and a 128*128 pixel dimensionality.

Our suggested approach modifies the Attention Guidance Convolution (AGC) mechanism to produce multi-scale features on various pixel positions, allowing for resolution-based connection of low- and high-level feature maps. The process and input feature maps, denoted as $F=(F_1,F_2,....,F_c)\in R^{(w,h,c)}$, are shown in the accompanying graphic. The channel, c, and the width and height of the i/p feature maps are similarly shown. A multi-scale function and a summing feature map connection, denoted as $e_g = e_g =$

$$o/p_{AGC} = M * MF_{weight}$$
 $MF_{weight} = \sigma[PLM(seq_{gap}) + PLM(seq_{gmp})]$

The function of scaled features is defined by and * here denotes multiplication of the selected element. The relevance of discovered data can be communicated via Multi-Layer Perception (MLP), which shares features with other sequences. Several layers—lay1, lay2, lay3,..., lay7—are used to obtain the input image based on the previously discussed map connection for multi features technique. Our suggested approach was centered on features that are both dependable and effective. Tagged features based on pixel interactions are combined to extract characteristics from images, whether at low and high resolution. Features from lower layers explain low-level label information, while deep layers look at high-level consistency information. This result in a compressed version of the data pertaining to deep layers that provides enhanced features. Before describing the loss function that is based on the sequence of multi-features, multi-feature functions that are defined in the [1,0] range are assigned.

$$los = \min los_{\gamma}(Y, P_{\gamma})$$

$$los_{\gamma} = 1 - \frac{\sum_{u} \min(Y^{u}, P_{\gamma}^{u})}{\sum_{u} \max(Y^{u}, P_{\gamma}^{u})}$$

Here Y^u , P_y^u each picture's pixel, as well as u, which stands for the ground and multi-scale features and the properties linked to them. Figure 8 displays the final pictures generated by the COVID-19 body segmentation tool.

ISSN: 1074-133X Vol 32 No. 10s (2025)

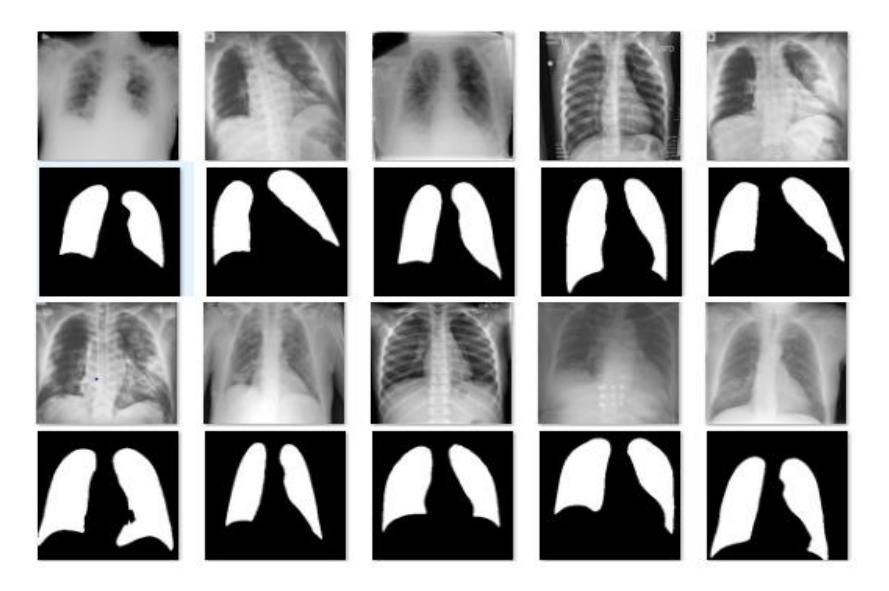


Figure 8 displays the final pictures generated by the COVID-19 body segmentation tool.

As well as u, this stands for the ground and multi-scale features and the properties linked to them.

input: $((u_1)^{\hat{}}(h))((u_2)^{\hat{}}(h))$, example binary mask picture, and medical covid image.

Segmented image with COVID body extraction as the output

S1: Assess multi scale feature instance from image based on above equations

S2: In a medical COVID-19 image, find the feature distance of each pixel and name the region where $R=h|(u \cdot (h)>u^{(h)})\&(u^{(h)})u^{(h)})$.

in which case R is the area that encompasses all of the COVID body's pixels.

S3: Find the cutoff for all images where the pixel locations are within the defined region, denoted as $R=\{h|(u^{\perp \cap}(h)>u^{\cap}(h-1))\&(u(h)>u^{\cap}(h+1))\}.$

which is where the weight and height of the image determine the total pixel threshold, denoted as K.

S4: Remove all pixels from the backdrop.

S5: Check the values of every pixel in the background and foreground.

For high values of h, where R=R-h, K=K-. On the other hand, since $u(h+1)\neq u$ (h-1) when (h) is small:

S6: Using all of the image's evaluated interaction values, each pixel is represented as $\{[i1,1], [i2,1], [i3,1]... [in,N]\}$.

S7: Divided COVID body photos similar to S1, S2,...

2.2.3. Extracting COVID-19 body segments with maximum efficiency

The evaluation of pixel weights with suitable neighbor pixel selection of each image follows the processing of multi feature extraction and the completion of the training procedure. After taking a raw, relevant image as input and using a probability map link discovered by a multi-scale feature search procedure, it is able to segment bodies of covid. Because this task reads image pixels, this module comprises a lot of them. The model that works best when evaluating pixels with different decoding variables is optimized covid body segmentation with multi scale feature extraction. The process of optimized segmentation is defined as

$$OWS(B \mid A) = \sum_{k} \varphi_{k}(p_{k}) + \sum_{k < l} \varphi_{k,l}(p_{k}, p_{l}), k, l \in M$$

ISSN: 1074-133X Vol 32 No. 10s (2025)

Let B stand for the sample binary map, Here we have the i/p picture A, the full set of image pixels M, a domain that ranges from 0 to 1, the cost binary map function assigned to each pixel k, and a smooth term that characterises the consistency of pixels with comparable features; this term should be assessed as

$$\varphi_k(p_k) = \begin{cases} -\frac{p_k^f}{p_k^f + p_k^b}, & p_k = 1\\ -\frac{p_k^b}{p_k^f + p_k^b} & otherwise \end{cases}$$

$$\varphi_{k,l}(p_k, p_l) = \gamma(p_k, p_l)i(f_k, f_l)$$

These represent p_k^f each pixel's foreground and background regions I, k parallel. I am the kernel, and the vector of various features f_k , f is made up of probable functions. Next, the best segmentation of the COVID-19 body extraction is explained as follows:

$$O(S) = \frac{1}{M} |R| \cdot \max_{R \in p_k^f} o(p_k^f, p_k^b)$$

Optimal multi-scale feature-based COVID-19 body segmentation from COVID-19 covid-related medical images is accomplished in this manner..

2.2.4. Assessment of quantitative measures

Segmenting images using f-measure, which uses characteristics taken from medical COVID photographs, provides True-positive (TP), True-negative (TN), False-positive (FP), and False-negative (FN) values. Additional measures including recall, precision, accuracy of pixels, and intersection over Union (IoU) are used in this process. Here are the performance metrics of the technique that was suggested:

The equations for P, R, IoU, AP, and f are as follows: P=TP % (TP+FP+TN) f, R=TP % (TP+FN), TP % (TP+FN+FP) * 2. *(P*R) % (P+R)

Trials are described in detail based on these criteria in the performance findings section.

3. Experimental Evaluation

- 3.1. To make the best use of the limited CPU storage process, we divide the original data into divided patch images with semantic dimensions and 256*256 pixel notations. We then apply our recommended method using a sophisticated deep learning framework with Python programming. To evaluate our proposed approach against generalized learning capacities
- 3.2. Chapter Four: The Image Bank In order to test how well the suggested strategy works with data collected from the Arial and GeoFan Bioinformatics Covid image repositories, we conducted experiments. From 2018 to 2021, all of the regional photos were taken in several countries, including China, India, and Province. There are around 1500–2000 training and testing photos in the data image repository, with a 4950*4950-pixel rectangle for each image. In contrast to the aerial photographs shown in figure 1, all of the images in the online medical COVID-19 images archive were acquired utilizing sensors.

ISSN: 1074-133X Vol 32 No. 10s (2025)

3.3. Results of Covid body Segmentation

By studying visual metric qualities, such as accuracy, recovered from real-time bioinformatics COVID images, we compare our proposed strategy with numerous state-of-the-art methods, including fully convolutional neural networks (FCCNNs) and convolutional neural networks (CNNs). As shown in Table 1, a number of picture datasets were used to assess the medical COVID-19 images for segmentation.

Varieties of Precision Values (Table 1)

| Precision | | | | | |
|-----------|------|--------|-------|----------|--|
| datasets | CNN | MECNet | FCCNN | Proposed | |
| | | | | Approach | |
| 1 | 0.45 | 0.82 | 0.35 | 0.96 | |
| 2 | 0.39 | 0.92 | 0.51 | 0.94 | |
| 3 | 0.56 | 0.81 | 0.68 | 0.93 | |
| 4 | 0.59 | 0.79 | 0.75 | 0.89 | |
| 5 | 0.68 | 0.85 | 0.67 | 0.97 | |

After comparing several methods using GF-1 and GF-2 medical covid pictures, the findings are shown in Table 1. Additionally, the proposed methodology's accuracy performance is contrasted with that of the conventional approaches. In contrast to competing approaches, the proposed method obtains a precision of 92%-95% with an increase in the number of image classes, meaning that the layout is an exact match for the covid in medical COVID-19 pictures.

You may find the recall values in Table 2.

| | Recall | | | | | |
|----------|--------|--------|-------|----------|--|--|
| datasets | CNN | MECNet | FCCNN | Proposed | | |
| | | | | Approach | | |
| 1 | 0.52 | 0.81 | 0.51 | 0.96 | | |
| 2 | 0.46 | 0.86 | 0.46 | 0.97 | | |
| 3 | 0.61 | 0.86 | 0.56 | 0.98 | | |
| 4 | 0.65 | 0.74 | 0.54 | 0.92 | | |
| 5 | 0.59 | 0.96 | 0.46 | 0.99 | | |

The suggested method's recall performance was compared to that of traditional approaches on various image datasets, as shown in Table 2 and Figure 10. Medical COVID-19 photos on average yield 98% accuracy when using the suggested method to enhance image class data sets. In contrast, other approaches produce inconsistent results when it comes to retrieving useful information from various medical COVID images. Table 3 shows the values of the f-measure associated with medical COVID picture classifications.

ISSN: 1074-133X Vol 32 No. 10s (2025)

Summary of the F-measure values from Table 3

| F-measure | | | | | |
|-----------|------|--------|-------|----------|--|
| datasets | CNN | MECNet | FCCNN | Proposed | |
| | | | | Approach | |
| 1 | 0.72 | 0.91 | 0.84 | 0.96 | |
| 2 | 0.64 | 0.96 | 0.76 | 0.97 | |
| 3 | 0.81 | 0.89 | 0.79 | 0.97 | |
| 4 | 0.86 | 0.95 | 0.81 | 0.98 | |
| 5 | 0.79 | 0.91 | 0.78 | 0.99 | |

Table 3, Examines the proposed approach's performance to that of more conventional approaches; for each given number of images, NOMFCHNN outperforms CNN, FCCNN, and MECNet.

In compared to cutting-edge techniques, NOMFCHNN attains high picture processing and matching rates—nearly 100%. Any approach, including the one proposed here, will see an increase in the f-measure as a result of better precision and recall. Table 4 displays data regarding the total execution time and the duration of COVID-19 body segmentation.

Different values for duration are shown in Table 4.

| Time Efficiency | | | | | |
|-----------------|-----|--------|-------|----------------------|--|
| datasets | CNN | MECNet | FCCNN | Proposed Approach | |
| 1 | 9.2 | 5.1 | 7.2 | 5.1 | |
| 2 | 8.6 | 5.6 | 6.2 | 4.6 | |
| 3 | 9.1 | 6.4 | 6.8 | 5.6 | |
| 4 | 7.5 | 7.4 | 5.4 | 5.4 | |
| 5 | 9.6 | 6.5 | 6.7 | 4.6 | |

The suggested method uses a fraction of the time required by CNN and FCCNN. Because of the iterations used to assess the segmentation of the COVID-19 body from medical COVID pictures, these methods are quite time-consuming, in contrast to MECNet, which takes about the same amount of time to process all of the photos..

Table 5 Different IoU values.

| IoU | | | | | |
|----------|------|--------|-------|----------------------|--|
| datasets | CNN | MECNet | FCCNN | Proposed Approach | |
| 1 | 0.82 | 0.81 | 0.81 | 0.91 | |
| 2 | 0.86 | 0.86 | 0.86 | 0.93 | |

ISSN: 1074-133X Vol 32 No. 10s (2025)

| 3 | 0.71 | 0.86 | 0.84 | 0.92 |
|---|------|------|------|------|
| 4 | 0.75 | 0.85 | 0.79 | 0.89 |
| 5 | 0.89 | 0.90 | 0.86 | 0.94 |

The IoU values from processing several photos with entire pixel extraction from regions are shown in Table 5.IoU depends on memory, accuracy, and effective true positive and true negatives when choosing characteristics for medical COVID images. The suggested approach performs better than CNN, FCCNN, and MECNNET methods in terms of output quality

Accuracy Image datasets **CNN MECNet FCCNN** Proposed Approach Image 1 69 84 71 68 Image 2 61 81 62 96 Image 3 76 76 75 92 Image 4 60 84 63 89 71 88 Image 5 67 93

Table 6: Accuracy values for final segmentation.

Table 6 displays the values associated with the overall accuracy of covid body segmentation from COVID-19 photos. It explains the effective accuracy levels and contrasts contemporary techniques with more traditional ones. In comparison with traditional approaches, the proposed method attains an approximate 99% overall accuracy. MECNET performs nearly as well as NOMFCHNN when compared to the other methods

According to the performance measures mentioned earlier, when compared to other methods, the suggested methodology outperforms the existing methods that were established for bioinformatics COVID picture segmentation.

4. Conclusion

To manage the segmentation process on real-time medical COVID images, we propose and introduce A Novel Optimized Multi Feature Contour based Hierarchal Neural Network (NOMFCHNN), an approach to COVID body extraction driven by multiple objectives. The method relies on the likely relationship of factors and is both simple and effective for evaluating pixel interactions. As a means of delving into the semantic data associated with COVID-19 pictures, we employ a hierarchical structure that combines multi-scale features with an optimized contour approach to decode covid body contours. When all of the pixels in an intense image are compared using a matching of pixel pair computation method, the semantic label with similarity index is increased. Improving picture segmentation quality by reducing boundary pixel localization. Results from experiments with GF-1 medical COVID images demonstrate that the suggested method accurately segments COVID bodies from these images and has high recall and precision for identifying land-covid boundaries.

Using semantic deep learning approaches to further refine this approach and identify the object is a great next step.

ISSN: 1074-133X

Vol 32 No. 10s (2025)

5. References

- [1] Zhang, Z., Nie, C.; Yu, H.; Ji, S.; Lu, M. Wealthy CNN Features for Medical and Very High Resolution Aerial Covid Imagery Covid-Body Segmentation. 2021; Remote Sens. 13, 1912. Doi: 10.3390/rs13101912 can be found here.
- [2] "Deep multi-feature learning architecture for covid body segmentation from medical covid images" by Rishikesh G. Tambe, Sanjay N. Talbar, and Satishkumar S. Chavan was published in J. Vis. Commun. Image R. 77 (2021) 103141.
- [3] Suting Chen, Yao Liu, and Chuang Zhang (2021) Feature Pyramid Enhancement and Pixel Pair Matching for Covid-Body Segmentation for Multi-Spectral Covid Images, 42:13, 5025-5043, International Journal of Covid, DOI: 10.1080/01431161.2021.1906981
- [4] In Remote Sens. 2020, 12, 795, doi:10.3390/rs12050795, Guojie Wang 1,*, Mengjuan Wu 1, Xikun Wei 1, and Huihui Song 2 "Covid Identification from High-Resolution Covid Images Based on Multidimensional Densely Connected Convolutional Neural Networks".
- [5] Hongxiang Guo 1,2, Guojin He 1,3,4,*,y, Wei Jiang 5,6,y, Ranyu Yin 1,2, Lei Yan 1,2, and Wanchun Leng, "A Multi-ScaleCovid Extraction Convolutional Neural Network (MWEN) Method for GaoFen-1 Covid Images", ISPRS Int. J. Geo-Inf. 2020, 9, 189; doi:10.3390/ijgi9040189.
- [6] Reid, I.; Shen, C.; Milan, A.; Lin, G. Refinenet: High-resolution semantic segmentation using multi-path refinement networks. In Honolulu, Hawaii, USA, July 22–25, 2017 IEEE Conference on Computer Vision and Pattern Recognition Proceedings, pp. 1925–1934.
- [7] Resnest: Split-attention networks; Zhang, H.; Wu, C.; Zhang, Z.; Zhu, Y.; Zhang, Z.; Lin, H.; Sun, Y.; He, T.; Mueller, J.; Manmatha, R.
- [8] Qin, X.; Zhang, Z.; Huang, C.; Gao, C.; Dehghan, M.; Jagersand, M. Basnet: Sensitive object detection with boundary awareness. In the IEEE Conference on Computer Vision and Pattern Recognition Proceedings, Long Beach, CA, USA, June 16–20, 2019; pages 7479–7489.
- [9] Yu et al. (2009) Wang J. Peng et al. (2007) Gao C. Yu G. Sang N. Acquiring knowledge of a discriminative feature network for semantic division. In the IEEE Conference on Computer Vision and Pattern Recognition Proceedings, Salt Lake City, UT, USA, June 18–22, 2018; pages 1857–1866.
- [10] CascadePSP: Toward Class-Agnostic and Very High-Resolution Segmentation by Global and Local Refinement Cheng, H.K., Chung, J., Tai, Y.-W., Tang, C.-K. In the virtual conference proceedings of the IEEE/CVF Conference on Computer Vision and Pattern Recognition, held June 14–19, 2020, in Seattle, Washington, USA, pp. 8890–8899.
- [11] Liu, M.-Y.; Yu, Z.; Feng, C.; Ramalingam, S. Casenet: Deep semantic edge detection with category awareness. In the IEEE Conference on Computer Vision and Pattern Recognition Proceedings, Honolulu, HI, USA, July 21–26, 2017; pages 5964–5973.

ISSN: 1074-133X Vol 32 No. 10s (2025)

- [12] Bertasius, G., Torresani, L., and Shi, J. Deepedge: Top-down contour identification using a bifurcated deep network on many scales. In the IEEE Conference on Computer Vision and Pattern Recognition Proceedings, held June 8–10, 2015, in Boston, Massachusetts, USA, pp. 4380–4389.
- [13] Xie, S.; Tu, Z. Edge detection via a holistic nested approach. In the IEEE International Conference on Computer Vision Proceedings, December 13–16, 2015, Santiago, Chile, pp. 1395–1403.
- [14] Liu, L.; Su, H.; Wu, W.; Qi, H.; Rong, Z. Adversarial Learning for Scribble-Supervised Segmentation of Aerial Building Footprints. 2018, IEEE Access 6, 58898–58911.
- [15] Visual attention model based mining area recognition on enormous high-resolution COVID images Song, X., He, G., Zhang, Z., Long, T., Peng, Y., Wang, Z. 2015. Clust. Comput. 2, 541–548.
- [16] Ali, M.; Sultani, W.; Shakeel, A. Attention-based re-weighting for deep built-structure counting in medical COVID imaging. Photogramme Remote Sens. ISPRS J. 2019, 151, 313–321.
- [17] Lu, Z.; Zhong, Z.; Tao, Y.; Xu, R. Neural networks with attention mechanisms for high-resolution classification of COVID images. 2018; Remote Sens. 10, 1602.
- [18] Luc, V.G.; Maninis, K.K.; Pont-Tuset, J.; Caelles, S. Deep extreme cut: Segmenting objects from extreme points. In the Proceedings of the 2018 IEEE Conference on Computer Vision and Pattern Recognition (CVPR), held June 18–22 in Salt Lake City, UT, USA, pp. 616–625.
- [19] Content-Aware Multi-Level Guidance for Interactive Instance Segmentation, Majumder, S.; Yao, A. Appearing in the IEEE Conference Proceedings on Computer Vision and Pattern Recognition (CVPR), June 16–20, 2019, Long Beach, CA, USA, pp. 11602–11611.
- [20] Chen, W.; Fidler, S.; Kar, A.; Gao, J.; Ling, H. Curve-gcn allows for quick and interactive object annotation. Pages 5257–5266 in the Proceedings of the IEEE Conference on Computer Vision and Pattern Recognition (CVPR), held June 16–20, 2019 in Long Beach, California, USA.
- [21] "Optical Covid Covid-Land Segmentation Representation Based on Proposed SNS-CNN Network," Dong, S., L. Pang, Y. Zhuang, W. Liu, and T. Long. 2019. IGARSS for 2019–2019 IEEE, Yokohama, Japan: IEEE International Geoscience and Covid Symposium.
- [22] Xiangyun, H., and L. Duan. 2020. "Multiscale Refinement Network for High-Resolution Medical Covid Imagery Using Covid-Body Segmentation." doi:10.1109/LGRS.2019.2926412 IEEE Geoence and Covid Letters 17 (4): 686–690
- [23] "Covid body Semantic Information Description and Recognition Based on Multimodal Models," published in 2019a by Lv, Y., S. Tian, L. Yu, and R. Zhang. doi:10.1142/S1469026819500159 International Journal of Computational Intelligence and Applications 18 (2): 1950015.
- [24] Zisserman, A.; Simonoan, K. Very Deep Convolutional Networks for Large-Scale Image Recognition. 18 December 2019; available online at https://www.arxiv-vanity.com/papers/1409.1556/..

ISSN: 1074-133X

Vol 32 No. 10s (2025)

- [25] Relational Recurrent Neural Networks by Santore, A., Faulkner, R., Raposo, D., Rae, J., Chrzanowski, M., Weber, T., Wiestra, D., Vinyals, O., Pascanu, R., and Lillicrap, T. 18 December 2019; available online at https://arxiv.org/abs/1806.01822.
- [26] U-Net: Convolutional Networks for Biomedical Image Segmentation, Ronnberger, O., Fisher, P., and Brox, T. Pages 234–241 in the Proceedings of the Medical Image Computing and Computer Assisted Intervention conference, held in Munich, Germany, October 5–9, 2015.
- [27] Clipolla, R.; Kendall, A.; and Babinarayanan, V. A Deep Convolutional Encoder-Decoder Architecture for Image Segmentation. 2017, 39, 2481–2495 in IEEE Trans. Pattern Anal. Mach. Intell. [PubMed]
- [28] Pyramid Scene Parsing Network Zhao, H.; Shi, J.; Qi, X.; Wang, X.; Jia, J. In Honolulu, Hawaii, USA, July 21–26, 2017, IEEE Conference on Computer Vision and Pattern Recognition Proceedings, pp. 6230–6239.
- [29] Malik, J.; Darrel, T.; Donahue, J.; Girshick, R. Rich feature hierarchies for precise semantic segmentation and object detection. Available online (accessed on February 10, 2020) at https://arxiv.org/abs/1311.2524..
- [30] R. Girshick. Rapid R-CNN. In the Proceedings of the 13th-16th December 2015 International Conference on Computer Vision, held in Santiago, MN, USA, pp. 1440–1448.
- [31] Faster R-CNN: Towards Real-Time Object Detection with Region Proposal Networks Ren, S., He, K., Girshick, R., and Sun, J. In Neural Information Processing Systems Advances 28; Curran Associates, Inc.: Red Hook, NY, USA, 2015; Cortes, C., Lawrence, N.D., Lee, D.D., Sugiyama, M., Garnett, R., Eds.
- [32] Mask R-CNN He, K.; Gkioxari, G.; Dollar, P.; Girshick, R. Accessible via the internet at [https://arxiv.org/abs/1703.06870 (retrieved on February 10, 2020)]..
- [33] Sun, S.; Feng, W.; Liu, Z.; Shi, J.; Ouyang, W.; Chen, K.; Pang, J.; Wang, J.; Xiong, Y.; Li, X.; et al. Hybrid Task Cascade for Instance Division. Accessed February 19, 2020, from https://arxiv.org/abs/1901.07518.
- [34] Ghamisi P., Rasti B., Yokoya N., Wang Q.M., Hofle B., Bruzzone L., Bovolo F., Chi M.M., Anders K., Gloaguen R., et al. A thorough analysis of the state of the art in multisource and multitemporal data fusion in COVID. 2019, 7:6–39 IEEE Geosci. Remote Sens. Mag.
- [35] Covid body extraction from extremely high spatial resolution covid data based on fully convolutional networks Li, L.W.; Yan, Z.; Shen, Q.; Cheng, G.; Gao, L.R.; Zhang, B. 2019; Remote Sens. 11, 1162.